AD-A108 567 STATE UNIV OF NEW YORK AT BUFFALO DEPT OF CHEMISTRY F/G 9/1
CHRONOAMPEROMETRIC TRANSIENTS AT THE STATIONARY DISK MICROELECT--ETC(U)
NOV 81 T HEPEL, J OSTERYOUNG N00014-79-C-0682
UNCLASSIFIED TR-7 NL

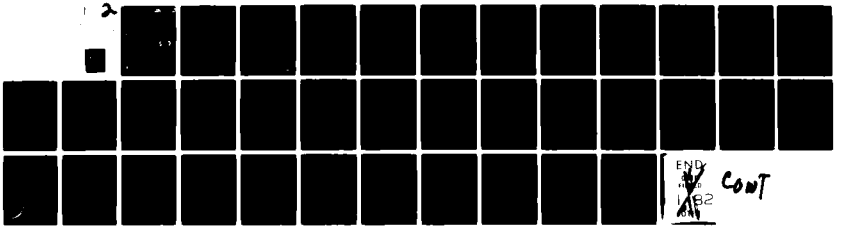

CONT

LEVEL II

12

SECURITY CLASSIFICATION OF THIS PAGE (When Data Entered)

REPORT DOCUMENTATION PAGE

READ INSTRUCTIONS BEFORE COMPLETING FORM

1. REPORT NUMBER: Technical Report No. 7	2. GOVT ACCESSION NO.: AD A108567
3. RECIPIENT'S CATALOG NUMBER	
4. TITLE (and Subtitle): Chronoamperometric transients at the Stationary Disk Microelectrode.	5. TYPE OF REPORT & PERIOD COVERED: Interim
	6. PERFORMING ORG. REPORT NUMBER
7. AUTHOR(s): Tadeusz Hepel and Janet Osteryoung	8. CONTRACT OR GRANT NUMBER(s): N00014-79-C-0682
9. PERFORMING ORGANIZATION NAME AND ADDRESS: Department of Chemistry, State University of New York at Buffalo, Buffalo, New York 14214	10. PROGRAM ELEMENT, PROJECT, TASK AREA & WORK UNIT NUMBERS: NR-056-715
11. CONTROLLING OFFICE NAME AND ADDRESS: Office of Naval Research/Chemistry Program, Arlington, Virginia 22217	12. REPORT DATE: November 30, 1981
	13. NUMBER OF PAGES: 29
14. MONITORING AGENCY NAME & ADDRESS(if different from Controlling Office)	15. SECURITY CLASS. (of this report): Unclassified
	15a. DECLASSIFICATION/DOWNGRADING SCHEDULE

16. DISTRIBUTION STATEMENT (of this Report)

Approved for Public Release: Distribution Unlimited

DTIC ELECTE DEC 15 1981 S D E

17. DISTRIBUTION STATEMENT (of the abstract entered in Block 20, if different from Report)

18. SUPPLEMENTARY NOTES

Prepared for publication in Journal of Physical Chemistry

19. KEY WORDS (Continue on reverse side if necessary and identify by block number)

Chronoamperometric transients; microelectrodes; diffusion coefficients

20. ABSTRACT (Continue on reverse side if necessary and identify by block number)

Chronoamperometric transients for diffusion controlled reactions at stationary platinum and gold microelectrodes have been examined. The results are compared with those predicted theoretically for hemispherical electrodes and for disk electrodes. The hemispherical model was found to describe the current-time transients only qualitatively, while excellent agreement was obtained between the theory for a stationary disk and data for the hexacyanoferrate (II)/(III) redox reaction. Equations for mass transport to a stationary disk electrode derived earlier form the basis for graphical methods of analysis of a (CONT.)

DD FORM 1 JAN 73 1473 EDITION OF 1 NOV 65 IS OBSOLETE

S/N 0102-LF-014-6601

SECURITY CLASSIFICATION OF THIS PAGE (When Data Entered)

AD A108567

DTIC FILE COPY

20. ABSTRACT: (Cont.)

single current-time transient which permit the simultaneous determination of two of the three parameters electrode radius, diffusion coefficient, and concentration. A plot of I vs. $t^{-1/2}$ has the advantage of simplicity. A logarithmic analysis (log I-log t) requires data over a greater time range but offers advantages in characterizing electrode geometry. The effects of surface irregularities and electrode sphericity are also discussed.

OFFICE OF NAVAL RESEARCH

Contract N00014-79-C-0682

Task No. NR-056-715

TECHNICAL REPORT NO. 7

CHRONOAMPEROMETRIC TRANSIENTS AT THE STATIONARY DISK MICROELECTRODE

by

TADEUSZ HEPEL AND JANET G. OSTERYOUNG

Accepted for Publication in

Journal of Physical Chemistry

Department of Chemistry
State University of New York at Buffalo
Buffalo, New York 14214

November, 1981

ABSTRACT

Chronoamperometric transients for diffusion controlled reactions at stationary platinum and gold microelectrodes have been examined. The results are compared with those predicted theoretically for hemispherical electrodes and for disk electrodes. The hemispherical model was found to describe the current-time transients only qualitatively, while excellent agreement was obtained between the theory for a stationary disk and data for the hexacyanoferrate(II)/(III) redox reaction. Equations for mass transport to a stationary disk electrode derived earlier form the basis for graphical methods of analysis of a single current-time transient which permit the simultaneous determination of two of the three parameters *electrode radius*, *diffusion coefficient*, *and concentration*. A plot of I vs. $t^{-1/2}$ has the advantage of simplicity. A logarithmic analysis (log I-log t) requires data over a greater time range but offers advantages in characterizing electrode geometry. The effects of surface irregularities and electrode sphericity are also discussed.

INTRODUCTION

Solid volammmetric electrodes of micrometer size have been found to have many advantages in comparison with large electrodes made of the same material.[1-12] The most important feature of micro-electrodes is the fact that the diffusion field increases in area with increasing distance from the electrode so markedly that the conversion of material by electrode reactions ceases to affect concentration profiles at rather short times. This results in the development of steady state currents at times which are experimentally convenient for avoiding mass transport by convection. The other feature is very low total electrode capacitance which allows for measurements of faradaic currents at very short times of electrolysis. Because of very small size, power requirements are minimized. The increasing interest in microelectrodes is also connected with many applications in which the electrodes have to be small, for example in bioengineering, medicine and microanalysis.

Microelectrodes of different shapes may be considered. Theory for diffusion control and charge transfer control for finite spherical electrodes has been developed in connection with polarographic applications. For a comprehensive review see Ref. 10. Electrochemical behavior at cylindrical electrodes has also been described.[10] In the latter case steady-state currents are not predicted. The solution of the diffusion problem for a circular planar microelectrode has been accomplished recently by Aoki and Osteryoung.[11] Some earlier attempts to describe this problem at stationary disks[3,13] produced equations

which disagree with digital simulation.[11,14,16]

In recent papers dealing with several aspects of voltammetry at microelectrodes, Dayton et al.[17,18] have used the hemispherical model for diffusion at carbon fiber microelectrodes. Though this model cannot describe quantitatively processes at planar electrodes, the effect of surface irregularities and some electrode sphericity may lead to experimental results similar to those predicted by the hemispherical model.

The theory of diffusion at finite disk electrodes derived elsewhere[11] has been verified experimentally for longer times[12] and very good agreement between the theoretical predictions and experimental results has been found. In this paper we investigate the theory for short times and extend measurements into the modified Cottrell region. A simple method of graphical analysis of experimental chronoamperometric transients allowing for simultaneous determination of the diffusion coefficient and the electrode surface area (or the concentration of reactant) is presented. The method of determining diffusion coefficients described before[12] is based on a complicated iterative numerical procedure and assumes knowledge of other parameters, such as electrode radius. The iterative method presented recently by Kakihana et al.[16] uses an approximate empirical expression for chronoamperometric curves derived from the results of digital simulations:

$$y = 1.7947 + 0.9979x + 0.4944\exp(-0.7246x) \qquad (1)$$

where

$x = r_0/\sqrt{Dt}$

$y = IFr_0nC°D/\sqrt{\pi}$

and r_0 is the radius of the electrode, D the diffusion coefficient of the diffusing species, t the time after pulse application at which the chronoamperometric current, I, is measured, n the number of electrons per molecule of reactant, F the faraday and C° the bulk concentration of diffusing material. Equation 1 is apparently valid for $r_0/\sqrt{Dt} \geq 2$. Again the treatment of data is unsatisfying because of complexity and lack of generality.

General treatment. The analytical solution on the problem of mass transport toward a stationary disk microelectrode under potentiostatic conditions[11] leads to the equations:

$$I = 4nFr_0DC°f(\tau')/(1 + \zeta) \qquad (2)$$

where ζ is given by the expression:

$$\zeta = (D_0/D_R)^{1/2} \exp\{(E-E^{\theta}) nF/RT\} \qquad (3)$$

Here E^{θ} is the formal potential for the reaction $O + ne \rightleftarrows R$, $D_0 \equiv D$ is the diffusion coefficient of O and D_R the diffusion coefficient of R. Below we consider quantitatively only data obtained under conditions where $\zeta \to 0$ and hence the current is independent of D_R. The function $f(\tau')$ in eq 2 has been given[11] in the form of an asymptotic series (small τ') and a descending series (large τ') where the dimensionless parameter τ' is given by $\tau' = 4Dt/r_0^2$.

When τ' approaches zero, I approaches the Cottrell current, $I_d = nFAC°\sqrt{D/\pi t}$, and when τ' approaches infinity, I approaches the steady-state current, $I_s = 4nFC°Dr_o$. For further analysis, we will use the dimensionless time τ which is slightly different from τ' and defined by

$$\tau = (16/\pi)Dt/r_o^2 \qquad (4)$$

The diffusion layer thickness under Cottrell control is $\delta_c = \sqrt{\pi Dt}$ while the steady-state diffusion layer thickness is $\delta_s = \pi r_o/4$. Thus $\tau = (\delta_c/\delta_s)^2$.

The equations for $f(\tau')$ of ref 11 may be expressed as functions of τ:

$$f_1(\tau) = f_1 = \frac{1}{\sqrt{\tau}} + \frac{\pi}{4} - \frac{3\pi^2}{2^{12}}\tau - \frac{315\pi^3\tau^2}{2^{25}} - \cdots \qquad (5)$$

and

$$f_2(\tau) = f_2 = 1 + \frac{4}{\pi^2\sqrt{\tau}} + 0.35412\tau^{-3/2} + 0.37875\tau^{-5/2} + \cdots \qquad (6)$$

To simplify the use of this solution (eq 5 and 6) we first produce a spliced equation good for all values of τ. The functions f_1 and f_2 (taken as above, without the remaining terms of the series) have two intersection points as shown in Figure 1. It is apparent from this figure that a good approximation for $f(\tau)$ may be obtained by assuming $f(\tau)$ changes from f_1 to f_2 somewhere in the range $2<\tau<5$. The difference in slope, $\partial f_1/\partial\tau - \partial f_2/\partial\tau$, at the intersection point at $\tau = 3.69$ is slightly less than that at $\tau = 2.03$, so that we use $\tau = 3.69$ as the cross-over point between f_1 and f_2. For further representation we use then for $f(\tau)$ the following expression:

$$f(\tau) = U(\tau-3.69)\ f_1 + [1-U(\tau-3.69)]f_2 \qquad (7)$$

where $U(\tau-3.69)$ is the Heaveside that has the value 1 for $\tau \leq 3.69$ and the value 0 for $\tau > 3.69$. The spliced $f(\tau)$-function, eq 7, is plotted in Figure 2.

According to the definition of τ (eq 4), the two limiting equations, i.e. the Cottrell equation and the steady-state equation, have an intersection point at $\tau = 1$ where $\delta_c = \delta_s$. As can be calculated from $\log f_1(\tau)$, the deviation of the logarithm of the actual current flowing through the microelectrode from the logarithm of the steady-state current is 0.250 at $\tau = 1$.

From eq 4

$$\log t = \gamma - \log D + 2 \log r_o \qquad (8)$$

where $\gamma = \log \tau + \log (\pi/16)$. The critical time, t_o, for which $\tau = 1$ depends on electrode radius and on the diffusion coefficient of the diffusing species:

$$\log t_o = \log(\pi/16) - \log D + 2 \log r_o \qquad (9)$$

From eq 5-7 one can also calculate the values of τ for which the current deviates from the limiting Cottrell or steady state current by a given percentage. These values of τ may be used in eq 8 to calculate values of t_s and t_c, the times at which the current deviates by a given fraction from the steady state or the Cottrell current, respectively. As the calculation of τ involves a tedious, iterative procedure, several examples calculated from eq 8 are plotted in Figure 3. Lines are

plotted for various values of D, and the values of τ and γ employed in the calculations are included in Table I. Figure 3 may be used to choose the electrode radius necessary to obtain steady-state currents at a given time or to see when deviations from the Cottrell equation become significant.

The previous experimental verification[12] of the theory[11] for stationary disk microelectrodes was carried out over the pertinent range of τ (0.005-25) but at rather long times (0.05-3 s). In the present work the time of current measurement is extended to values as small as 130 μs and to values of τ as small as 0.001. The electrode construction was chosen to make possible measurements at such short times. In order to check the accuracy of the spliced function $f(\tau)$ (eq 7) logarithmic analysis (log I vs. log t) was performed to investigate chronoamperometric relations over a wide range of elapsed time.

EXPERIMENTAL SECTION

Solutions were prepared using chemicals of reagent grade purity (without further purification) and deionized water (18 MΩ cm, Milli-Q purification system).

The electrodes were constructed using fine metal wires. A platinum wire of 0.2 mm diameter was carefully polished with polishing powders of decreasing size down to 0.3 μm (Dry Powder, Type A, Fisher Scientific Co.) using a polishing cloth (Fisher, 12-28, 2B). The resulting thin wire was etched in concentrated nitric acid, reduced in sulfuric acid under cathodic bias with simultaneous copious evolution of hydrogen,

washed with deionized water and dried at room temperature. The Pt wire was then soldered to a thick copper wire (diameter 0.5 mm), and the junction was etched with acetone and ethyl alcohol. The electrolytic reduction of surface platinum oxides was then repeated. The gold wires were prepared similarly. However, after mechanical polishing an electrolytic dissolution in an alkaline cyanide bath was carried out. Each fine metal wire thus obtained was embedded with epoxy resin into a glass tube of external diameter at least 8 mm (in order to avoid edge effects). The top of the glass tube was polished to obtain a flat surface. The active area of these disk-electrodes was in the range 3×10^{-6} - 1.2×10^{-5} cm^2 (the electrode radii 11-50 μm). The active electrode was located approximately in the center of the top of a glass holder. Before each experiment the electrodes were conditioned in 0.1M H_2SO_4 under cathodic bias (E = -340 mV vs. SCE) for 10 minutes, cycled between the potentials of oxygen and hydrogen evolution and reduced at E = -340 mV for 15 min.

A conventional three electrode design was used for measurements. A platinum coil and saturated (KCl) calomel electrode were used as the counter- and reference-electrodes, respectively. All potentials are reported vs. SCE. Experiments were performed at 27°C.

The electronic set-up consisted of a Tacussel pulse unit, Model UAP-4; PARC Model 173 (Princeton Applied Research) and Tacussel Model PRG-3 potentiostats; Biomation Model 8100 fast 8-bit analog to digital converter with 2024 K-word memory; Tektronix Model 603-A storage oscilloscope and Hewlett-Packard Model 7046A XY plotter.

The sampling time was 1 or 5 μs for short-time measurements. In some longer-time measurements sampling times in the range 50 μs to 5 ms were also used.

RESULTS AND DISCUSSION

Applicability of eq 5-7 for chronoamperometry at stationary disk microelectrodes was checked using the hexacyanoferrate(II)/(III) redox reactions at the platinum and gold electrodes. The range of potentials where diffusion controlled currents flow through the electrode was established on the basis of linear-sweep and normal-pulse voltammetric characteristics. An example of the normal pulse voltammetric curves obtained for the oxidation of ferrocyanide at a gold microelectrode is shown in Figure 4 for the range of pulse widths 2.5 to 9 ms and sampling time 5 μs at the end of the pulse. Pulses of such short duration could be applied because of very low electrode capacitance. In addition IR compensation by positive feedback was employed using the UAP-4 pulse unit.

The values of the electrode potentials selected on the basis of the normal pulse experiments were in the range +280 to +340 mV and each new electrode prepared was tested at these potentials (usually +320 mV). For the conditioning potential the value -100 mV was used. After each measurement the solution was extensively stirred by argon bubbling for 10 min. This was followed by a 20-min delay to minimize convection. Typical direct chronoamperometric characteristics obtained for oxidation of ferrocyanide at a gold microelectrode with radius 13.4 μm are presented

in Figure 5 for several values of electrode potential. The deviations from the Cottrell equation at short and medium times are shown in Figure 6 in which the experimental results (circles) and the theoretical lines are plotted in the coordinates $I\text{-}t^{-1/2}$.

In the coordinates $I\text{-}t^{-1/2}$ the line for the Cottrell current (1) is not an asymptote for the real current (2). Instead, curves (1) and (2) become parallel at short times. From analysis of eq 5-7 one can state that: 1) extrapolation of the short-time part of the $I\text{-}t^{-1/2}$ curve for the disk electrode to the ordinate gives the intercept $\pi I_s/4$; 2) the linear extrapolation of the real current (2') is shifted from the Cottrell line by $\sqrt{\pi D}/r_o$ along the abscissa toward smaller values of $t^{-1/2}$; 3) the slope of the experimental line at shorter times is $r_o I_s \sqrt{\pi}/4\sqrt{D}$. Using any two of these three quantities, one can determine simultaneously from one plot two of the three quantities: C°, r_o, and D.

It is also instructive to examine the relative deviation from the Cottrell current. This is easily obtained from eq 5, which can be presented in the form

$$I = nFDC^\circ A(1 + \zeta)^{-1}(\pi Dt)^{1/2}[1 + \pi\sqrt{\tau}/4 - 3\pi^2\tau^{3/2}/2^{12} - 315\pi^3\tau^{5/2}/2^{25} - \cdots] \qquad (10)$$

Thus

$$(I\text{-}I_d)/I_d = \pi\sqrt{\tau}/4 - 3\pi^2\tau^{3/2}/2^{12} - 315\pi^3\tau^{5/2}/2^{25} - \cdots \qquad (11)$$

Equations 9 and 10 are valid for $\tau \leq 3.69$. For small values of τ the first term on the righthand side of eq 10 is the most important, so

the lefthand side may be plotted versus $\sqrt{\tau}$ with initial slope (i.e. at τ = 0) equal to $\pi/4$. Such a plot is presented in Figure 5. Because the relative deviation depends only on τ, all the experimental results can be represented in this plot. As can be seen the agreement between theory and experiments is excellent. Small deviations from the theoretical line observed for some electrodes may be due to irregularities of the electrode surface.

The entire measurement range of the chronoamperometric characteristics, which consists of several separate experiments, is illustrated in Figure 8 for three gold electrodes with radii 11.0, 13.4 and 19.0 μm. As in the case of the I-$t^{-1/2}$ plot, from this log I-log t plot the diffusion coefficient and the electrode surface area (or concentration C°) can be determined simultaneously. In analogy with Figure 2, we have $\partial \log I_d / \partial \log t = 0.5$ and $\partial \log I_s / \partial \log t = 0$. In addition, at $t = t_o$, $\log I - \log I_s = \log I - \log I_d = 0.250$. Using these relations we can obtain graphically from the log I vs. log t plot the quantities I_d and I_s, and hence $r_o D^{1/2}$ and $r_o D$, respectively. These two are sufficient to estimate r_o and D. If they are correct, the appropriate value of t_o should be obtained from eq 9. This test is very sensitive to even small errors in r_o and D. Such errors may come from incorrect estimation of the limiting Cottrell line when the electrode is very small (compare Figure 3) or from convection and mechanical vibrations of the measurement cell which influence the limiting current, especially when measured at longer times (larger electrodes). If the metal microelectrode is embedded in relatively soft material and then is polished using dry

polishing powders, the chronoamperometric transients are characterized by a greater value of t_0 and higher currents in the Cottrell region as well as in the steady-state domain. This effect may be due to some sphericity of the electrode shape. In Figure 9 the experimental curve 3 obtained after dry polishing lies nearer to the theoretical curve 2 for a hemispherical electrode than to the curve 1 for a disk electrode. The usual definition of the reduced time parameter for hemispherical diffusion is $\tau'' = \pi Dt/r^2$. However, for purposes of comparison we use τ as defined by eq 6 and thus the current for hemispherical diffusion is given by

$$I_h = 4nFDC^{\circ}(1 + \zeta)^{-1} r_0 (2/\sqrt{\tau} + \pi/2) \qquad (12)$$

As seen in Figure 1 the linear parts of curve 2 are shifted with respect to curve 1 in the Cottrell region by 0.301 (=log 2) and in the steady-state region by 0.196 (=log $\pi/2$) toward higher currents. In order to minimize the values of t_0 and t_s, flat electrodes should be constructed. Furthermore, because the current is so sensitive to geometry, it is essential to verify that the planar geometry is achieved if measurements similar to those of Figures 6 and 8 are used to obtain values of diffusion coefficients.

Table II presents results obtained from logarithmic analysis of chronoamperometric data at various electrodes. The precision of the values of r_0 and D for a single electrode is attained by rejecting data giving different values of t_0. The accuracy of the determination of electrode radius can be assessed by comparing the values obtained with the "true" values obtained by direct measurement. This good agreement

taken together with the remarkable precision in the values of D shows that chronoamperometric transients can be used reliably to determine the flatness and size of microelectrodes. The precision of the values of D over a five-fold range of electrode radius and ten-fold range of concentration argues well for the accuracy of the result. The value (7.94 $\pm$ 0.06) x 10^{-6} cm^2/s for hexacyanoferrate(II) may be compared with the value of (7.84 $\pm$ 0.02) x 10^{-6} cm^2/s obtained by Sato, et al. for hexacyanoferrate(III).[16] Also, Aoki and Osteryoung obtained the value 6.8 x 10^{-6} cm^2/s for hexacyanoferrate(II) with an estimate that the error was 10% or less.[12]

In this work we have emphasized the use of the current-time transient to assess electrode geometry and measure electrode size and to determine diffusion coefficients. As noted above, provided either r_o or D is known these techniques can be used to determine concentration. Applications of special interest are determination of electroactive species at high concentrations and determination of electroactive species in highly resistive solutions. The ability to operate at very short times without unusual power requirements should make these electrodes useful also for kinetic studies.

REFERENCES

(1) A. J. Bard and L. E. Faulkner, "Electrochemical Methods", Wiley and Sons, New York 1980, p. 151.

(2) A. J. Bard, Anal. Chem., 33, 11 (1961).

(3) Z. G. Soos and P. J. Lingane, J. Phys. Chem., 68 3821 (1964).

(4) R. N. Adams, Anal. Chem., 48 1129 (1976).

(5) P. T. Kissinger, C. Refshauge, R. Dveiling and R. N. Adams, Anal. Lett., 6 465 (1973).

(6) P. T. Kissinger, J. B. Hart and R. N. Adams, Brain Res., 55 209 (1973).

(7) C. A. Marsden, J. Conti, E. Strope, G. Curzen and R. N. Adams, Brain Res., 171 85 (1979).

(8) H. Y. Cheng, J. Schenk, R. Huff and R. N. Adams, J. Electroanal. Chem., 100 23 (1979).

(9) R. S. Picard, J Neuroscience Methods, 1 301 (1979).

(10) Z. Galus, "Fundamentals of Electrochemical Analysis", Ellis Harwood, Chichester 1976.

(11) K. Aoki and Janet Osteryoung, J. Electroanal. Chem., 122 11 (1981).

(12) K. Aoki and Janet Osteryoung, J. Electroanal. Chem., 125 315 (1981).

(13) S. Sarangapani, and R. J. DeLevie, J. Electroanal. Chem., 120 1650 (1979).

(14) J. B. Flanagan and L. Marcoux, J. Phys. Chem., 77 1051 (1953).

(15) M. Kakihana, H. Ikeuchi and G. P. Sato, J. Electroanal. Chem., 117 201 (1981).

(16) M. Kakihana, H. Ikeuchi, G. P. Sato and K. Tokudo, J. Electroanal. Chem., 108 381 (1980).

(17) M. A. Dayton, A. G. Ewing and R. M. Wightman, Anal. Chem., 52 2392 (1980).

(18) M. A. Dayton, J. C. Brown, K. J. Stutts and R. M. Wightman, Anal. Chem. 52 946 (1980).

(19) J.-L. Ponchon, R. Cespuglio, F. Gonon, M. Jouret and J.-F. Pujol, Anal. Chem., 51 1483 (1979).

FIGURE CAPTIONS

Fig. 1. Logarithmic plot of functions f_1 and f_2 vs. dimensionless time τ (f_1 - eq 7 for asymptotic expansion, f_2 - eq 8 for descending series).

Fig. 2. Dependence of the logarithm of the spliced function f (eq 9) on log τ. The limiting Cottrell function f_c intersects with the steady-state function f_s at $\tau = 1$.

Fig. 3. The relation between the critical time t_o (for equal deviations from the Cottrell currents and steady-state currents), and times t_s and time t_c for 1% deviation and the electrode radius, r_o, for various values of the diffusion coefficient: (1)) 4×10^{-6}, (2) 6×10^{-6}, (3) 8×10^{-6}, (4) 1×10^{-5}, (5) 1.2×10^{-5} $cm^2 s^{-1}$.

Fig. 4. Normal pulse voltammograms for oxidation of $Fe(CN)_6^{4-}$ on a stationary disk microelectrode. Sampling time: 5 μs; pulse width 2.5 to 9 ms as labeled; sweep rate 0.2 mV/s; $C^\circ = 5.36 \times 10^{-2}$ M in 0.5 M K_2SO_4; electrode: Au, r_o = 11.2 μm.

Fig. 5. Typical chronoamperometric transients at a gold stationary-disk electrode (r_o = 13.4 μm) in 5×10^{-3} M $Fe(CN)_6^{4-}$ and 0.5 M K_2SO_4. Conditioning potential: -100 mV. Pulse amplitude as labeled.

Fig. 6. Chronoamperometric limiting current transient of Figure 5 in the coordinates $I\text{-}t^{-1/2}$. Circles - experimental points, curve 1 - eq 9, curve 2 - extrapolation of the short-time part of experimental curve, line 3 - calculated from Cottrell equation for infinite planar electrode (of the same surface area).

Fig. 7. Relative deviation from the Cottrell current $(I-I_{d,c})/-I_{d,c}$ vs. $\sqrt{\tau}$. Experimental results obtained for gold electrode with r_o = 11.2 μm (open circles) and for platinum electrode, r_o = 26.1 μm (filled circles); solid line - eq 12; dashed line - initial slope (at $\sqrt{\tau}$ = 0) equal to $\pi/4$.

Fig. 8. Potentiostatic transients at Au microelectrodes over a wide range of elapsed time using logarithmic coordinates. Sloped dashed lines correspond to the Cottrell currents and horizontal ones to the steady-state currents. Curves 1-3 were calculated from eq 7-9 for r_o: (1) 11.2 μm, (2) 13.4 μm and (3) 19.6 μm. Circles are experimental results for oxidation of $Fe(CN)_6^{4-}$ (5×10^{-3} M) in 0.5 M K_2SO_4.

Fig. 9. Effect of electrode sphericity and surface irregularities on chronoamperometric transient. Curve 1 - eq 9 for disk electrode, curve 2 - eq 14 for hemispherical model and curve 3 - experimental, for electrode repolished with dry powder; r_o = 19.6 μm.

TABLE I

Values of the Parameter γ for Equation 10*

Deviation from, % Cottrell current	Deviation from, % steady-state current	τ	γ
1	-	1.62×10^{-4}	-12.4975
10	-	1.62×10^{-2}	-10.4975
20	-	6.49×10^{-2}	- 9.8947
77.82	77.82	1.	- 8.7070
-	20	5.73	- 7.9488
-	10	1.815×10^{1}	- 7.4481
-	1	1.640×10^{3}	- 5.4921

*r_o in μm, t in s, D in cm^2/s

TABLE II

Values of Diffusion Coefficient and Electrode Radius determined according to the procedure of Figure 8.

Electrode	$C^\circ \times 10^3$, M[a]	r_o, μm[b]	$\bar{r}_o$, μm[c]	$D \times 10^6$, cm^2/s	log t_o,(s)[d]	log t_o,(s)[e]
1-Au	53.6	11.0	11.2	7.84	-1.518	-1.55
	5.00	11.3		7.93	-1.500	-1.58
	0.92	11.3		7.91	-1.499	-1.54
2-Au	50.4	13.4	13.4	7.93	-1.352	-1.36
	5.00	13.3		7.92	-1.361	-1.37
	0.80	13.5		7.95	-1.347	-1.36
3-Au	51.1	19.8	19.6	7.99	-1.016	-1.02
	5.00	19.4		7.93	-1.031	-1.03
	0.83	19.7		7.97	-1.019	-1.03
4-Pt	49.9	23.7	23.8	8.05	-0.863	-0.86
	5.01	23.6		7.94	-0.861	-0.86
	0.40	24.0		8.04	-0.852	-0.86
5-Pt	53.6	26.0	26.1	7.82	-0.770	-0.79
	4.99	26.2		7.97	-0.772	-0.78
	0.40	26.1		7.90	-0.771	-0.78
6-Pt	50.0	48.9	48.8	7.91	-0.226	-0.22
	4.98	48.9		7.96	-0.229	-0.23
	0.40	48.6		7.89	-0.231	-0.23
			Average:	7.94 ± 0.06		

Table II (continued)

[a] concentration of $Fe(CN)_6^{4-}$ in 0.5 M K_2SO_4

[b] determined graphically

[c] determined by direct measurement

[d] calculated from eq 11

[e] estimated from the condition log I - log I_s = 0.250

ACKNOWLEDGMENT

This work was supported in part by the Office of Naval Research.

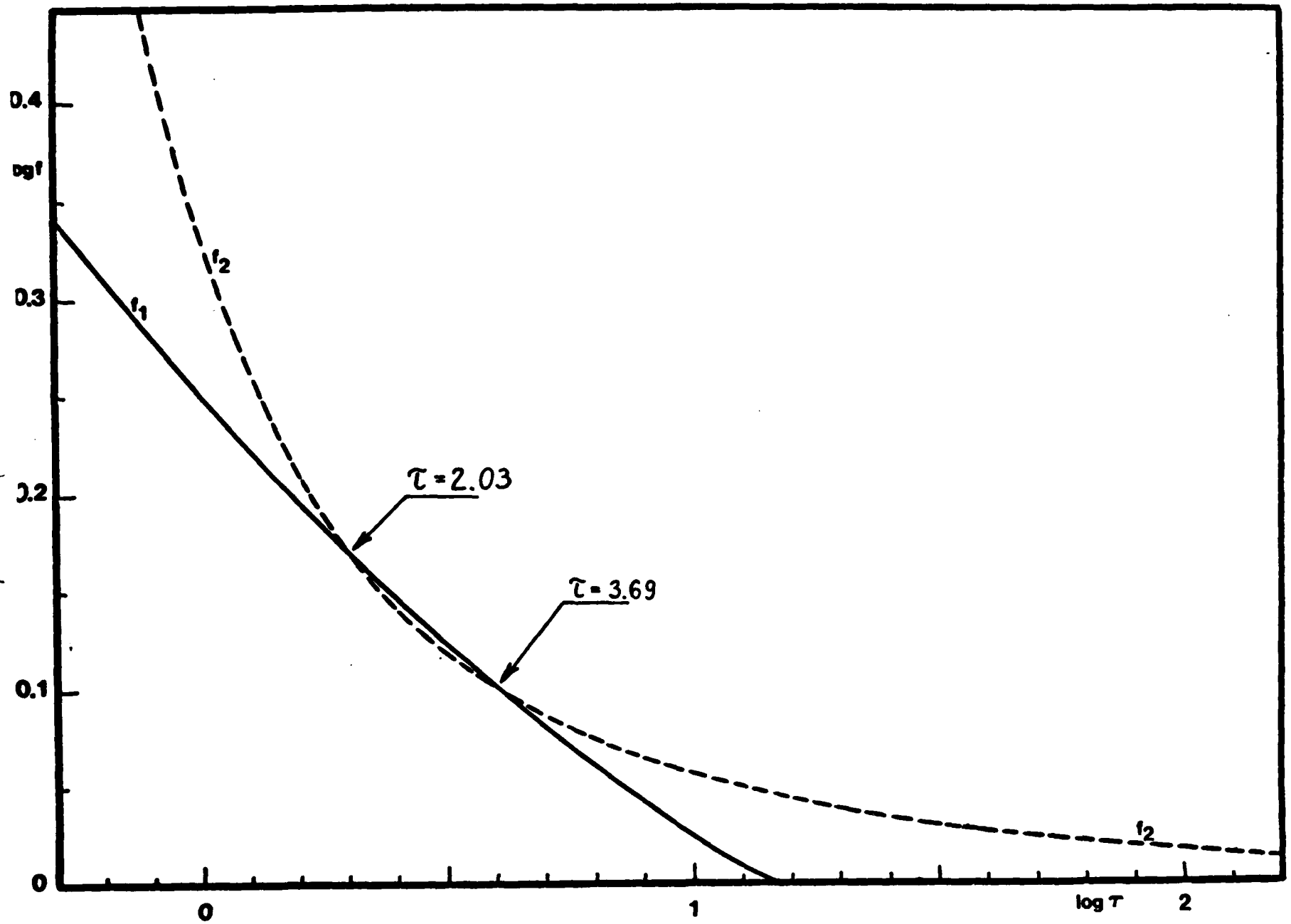

FIGURE 1

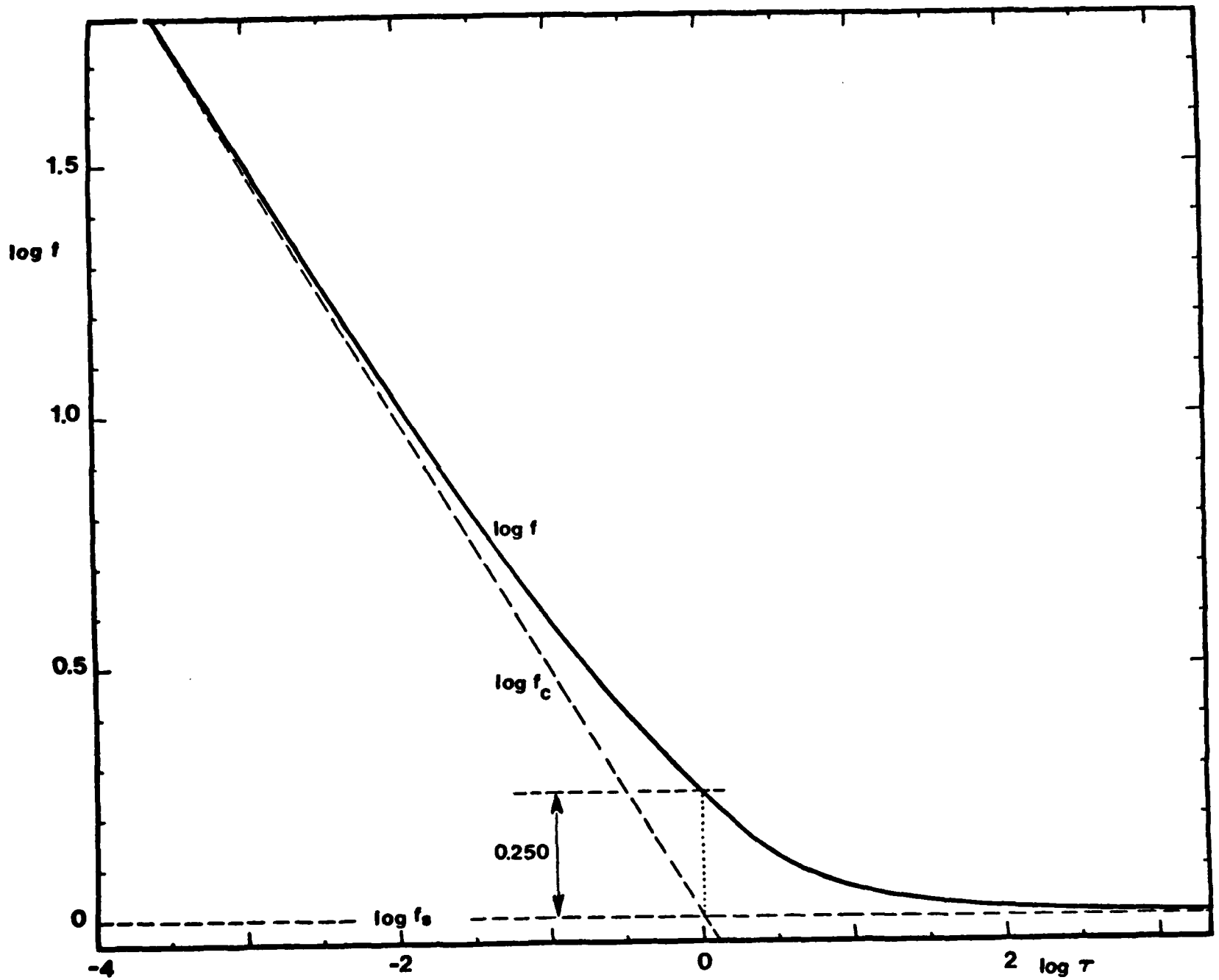

FIGURE 2

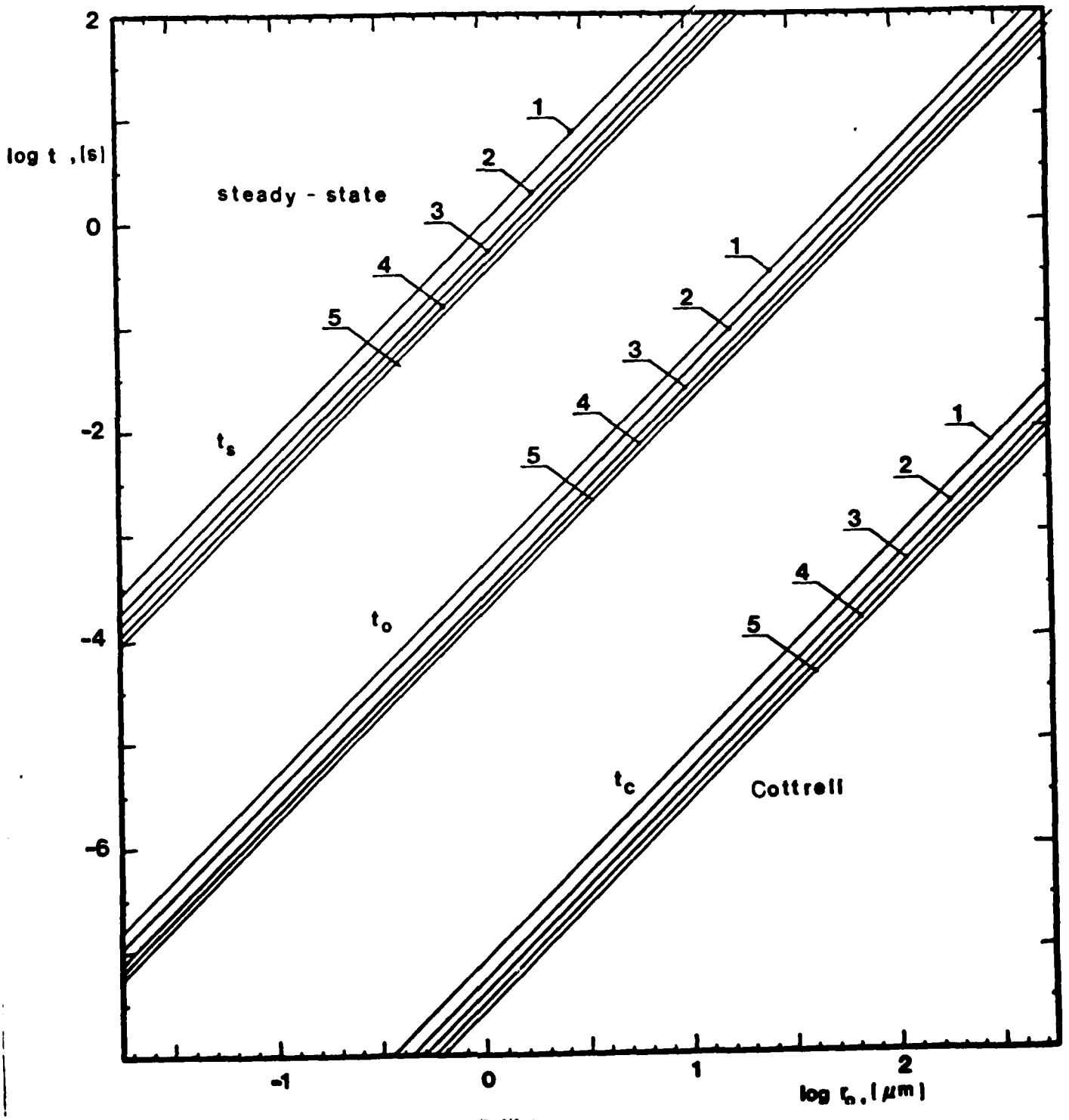
2
0
-2
-4
-6
log t ,[s]
steady - state
1
2
3
4
5
t_s
t_o
t_c
Cottrell
-1
0
1
2
log r_o,[μm]

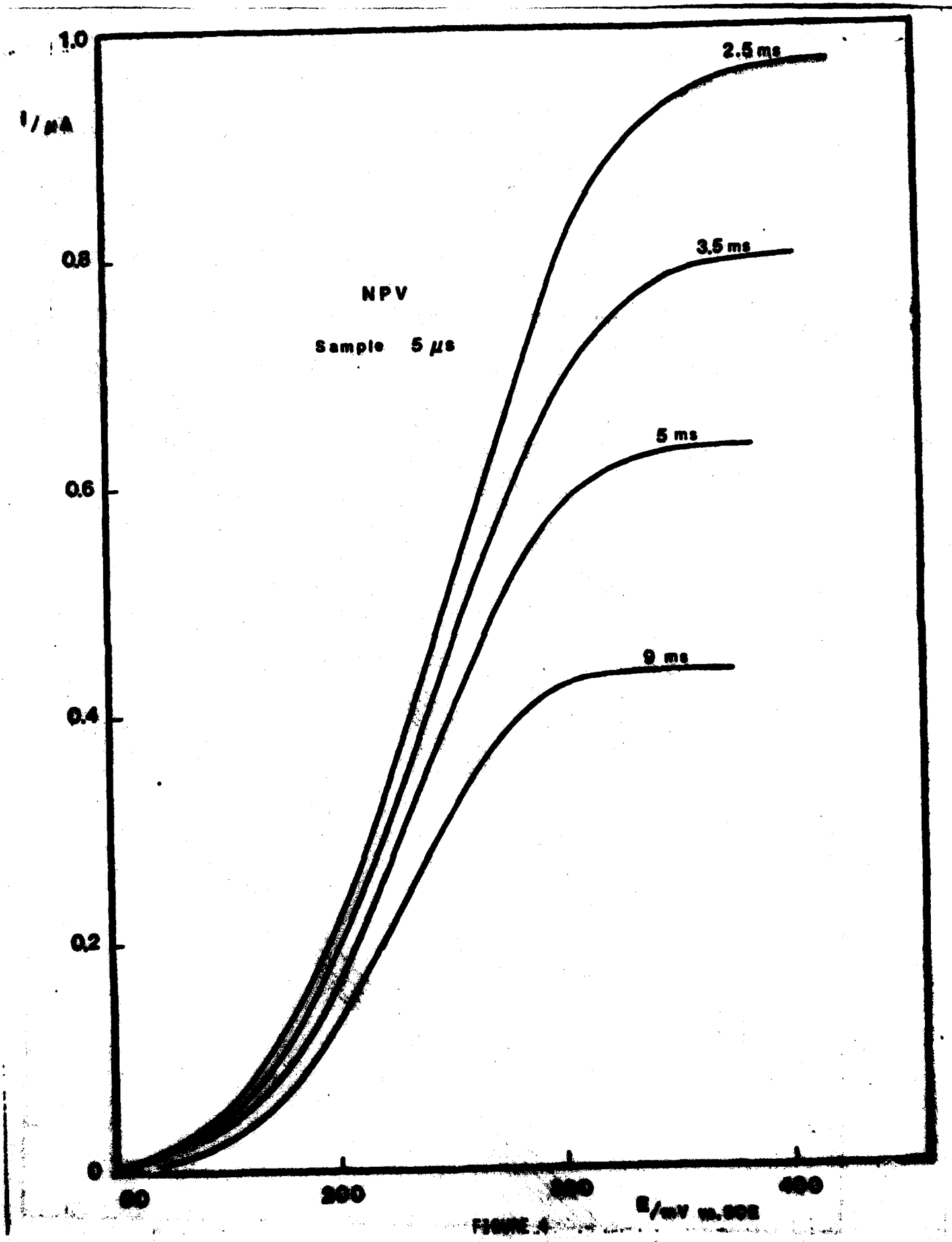
1.0
I / μA
0.8
0.6
0.4
0.2
0
2.5 ms
3.5 ms
5 ms
9 ms
NPV
Sample 5 μs
200
400
E/mV vs.SCE

FIGURE 4

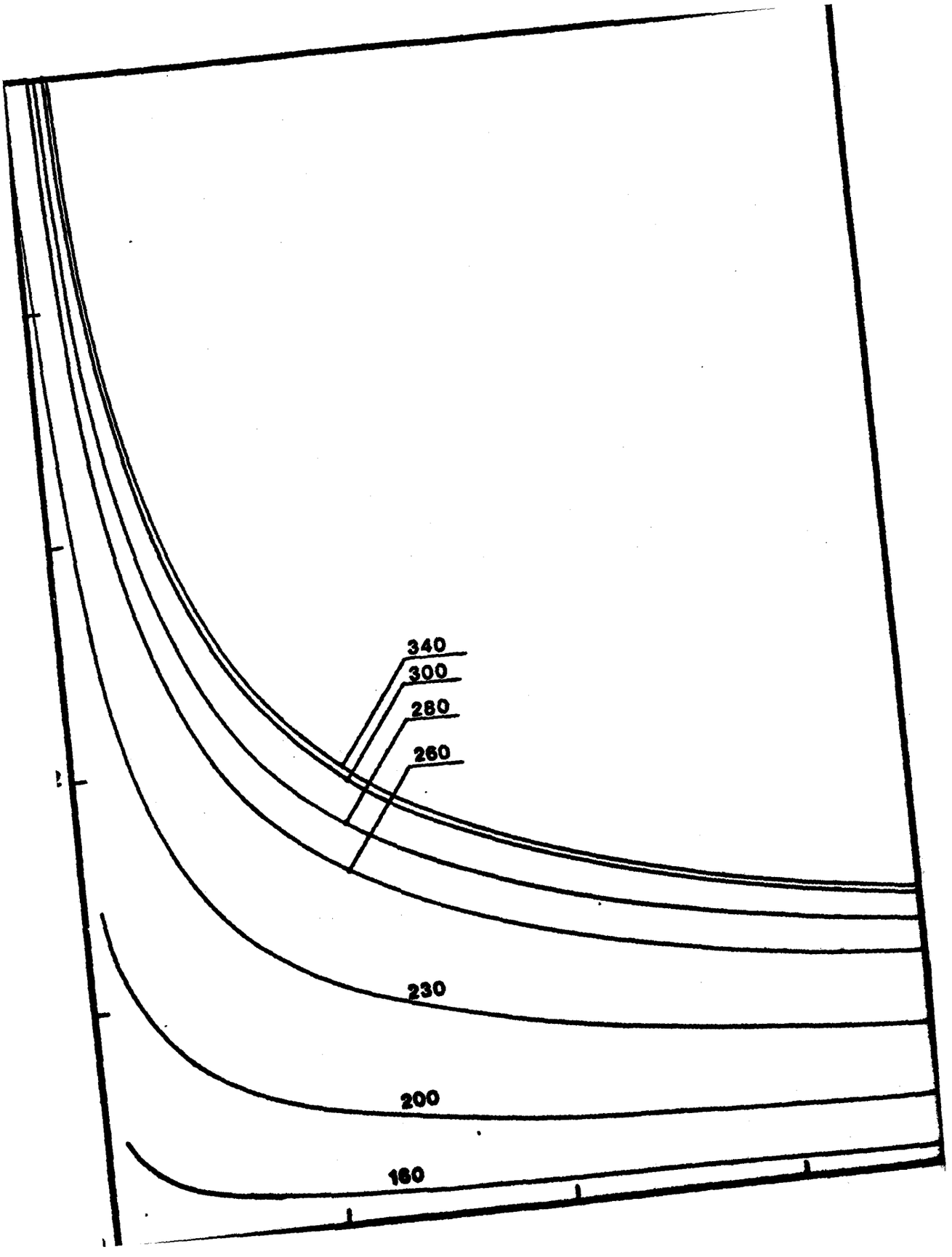
340
300
280
260
230
200
160

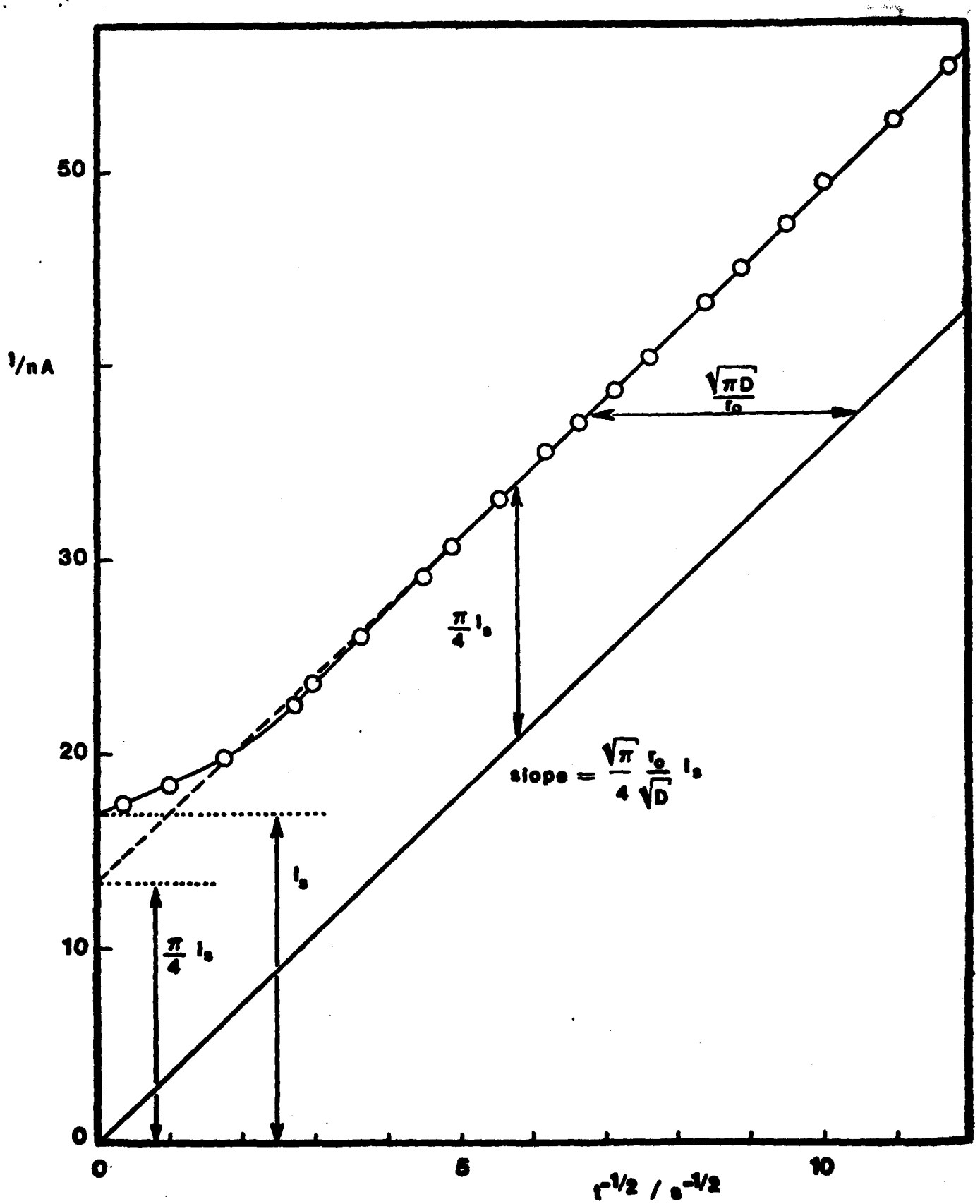
50
30
20
10
0
I/nA
0
5
10
$t^{-1/2}$ / $s^{-1/2}$
$\frac{\sqrt{\pi D}}{r_o}$
$\frac{\pi}{4} I_s$
I_s
$\frac{\pi}{4} I_s$
slope = $\frac{\sqrt{\pi}}{4} \frac{r_o}{\sqrt{D}} I_s$

FIGURE 6

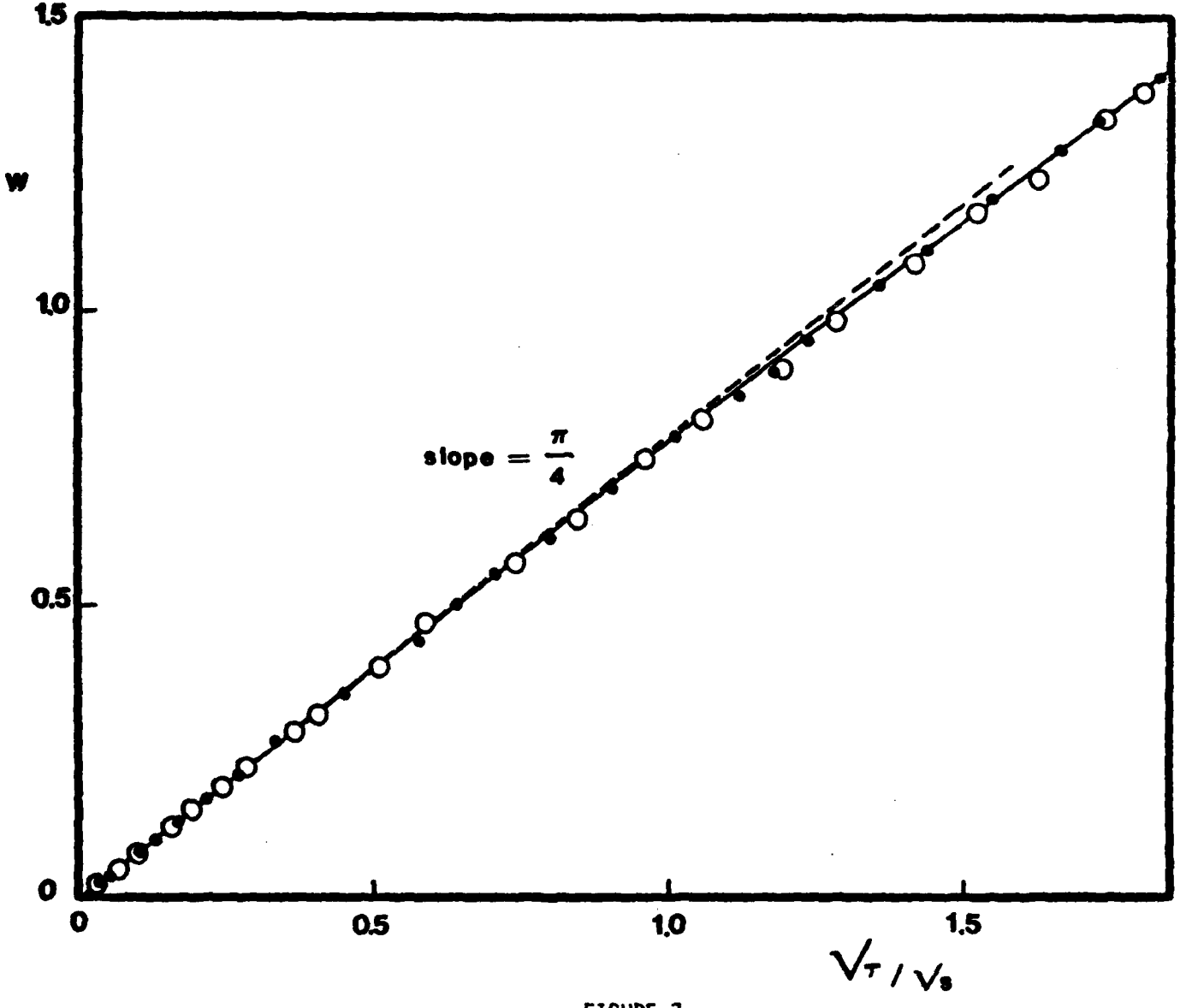

FIGURE 7

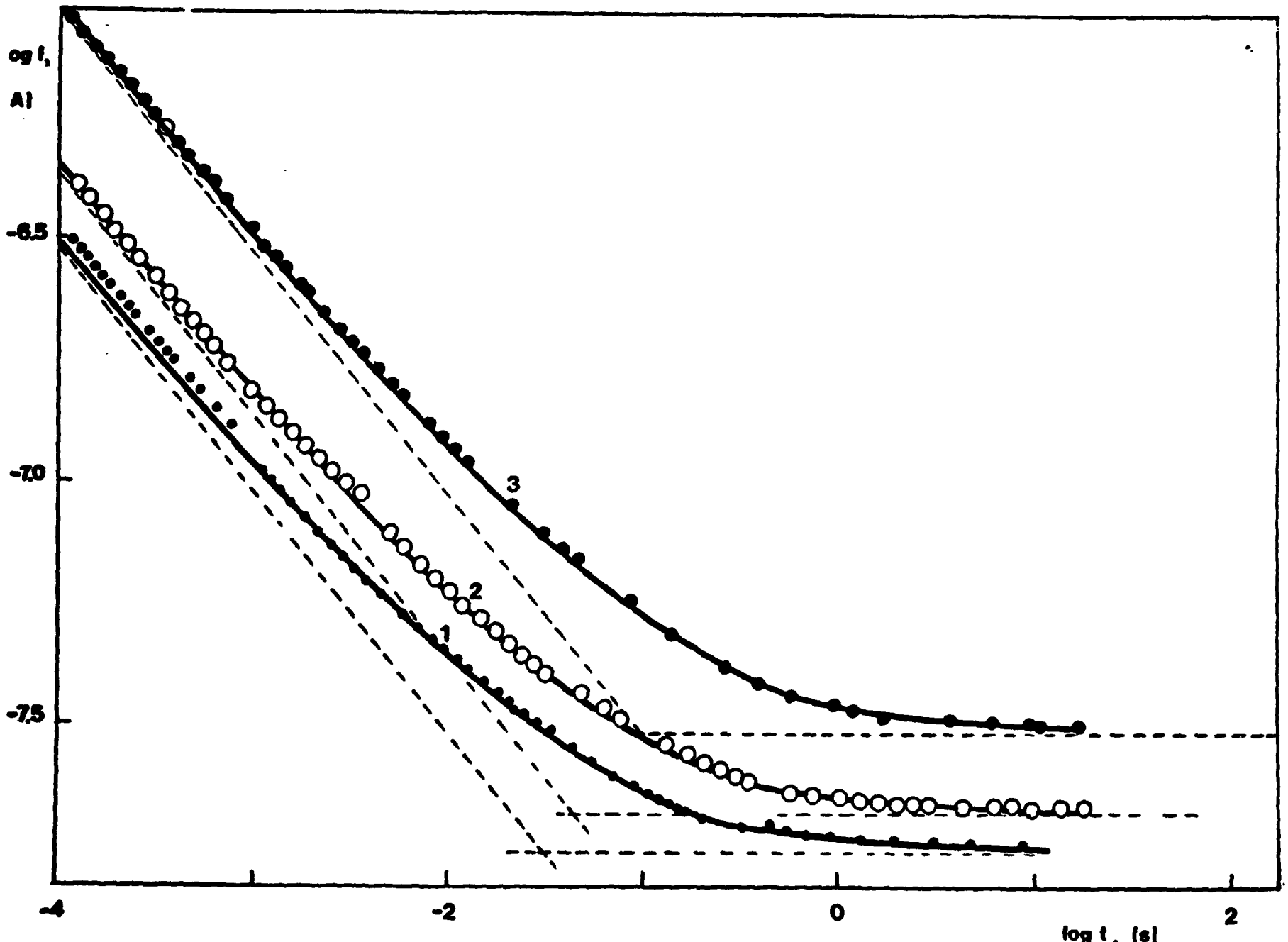

FIGURE 8

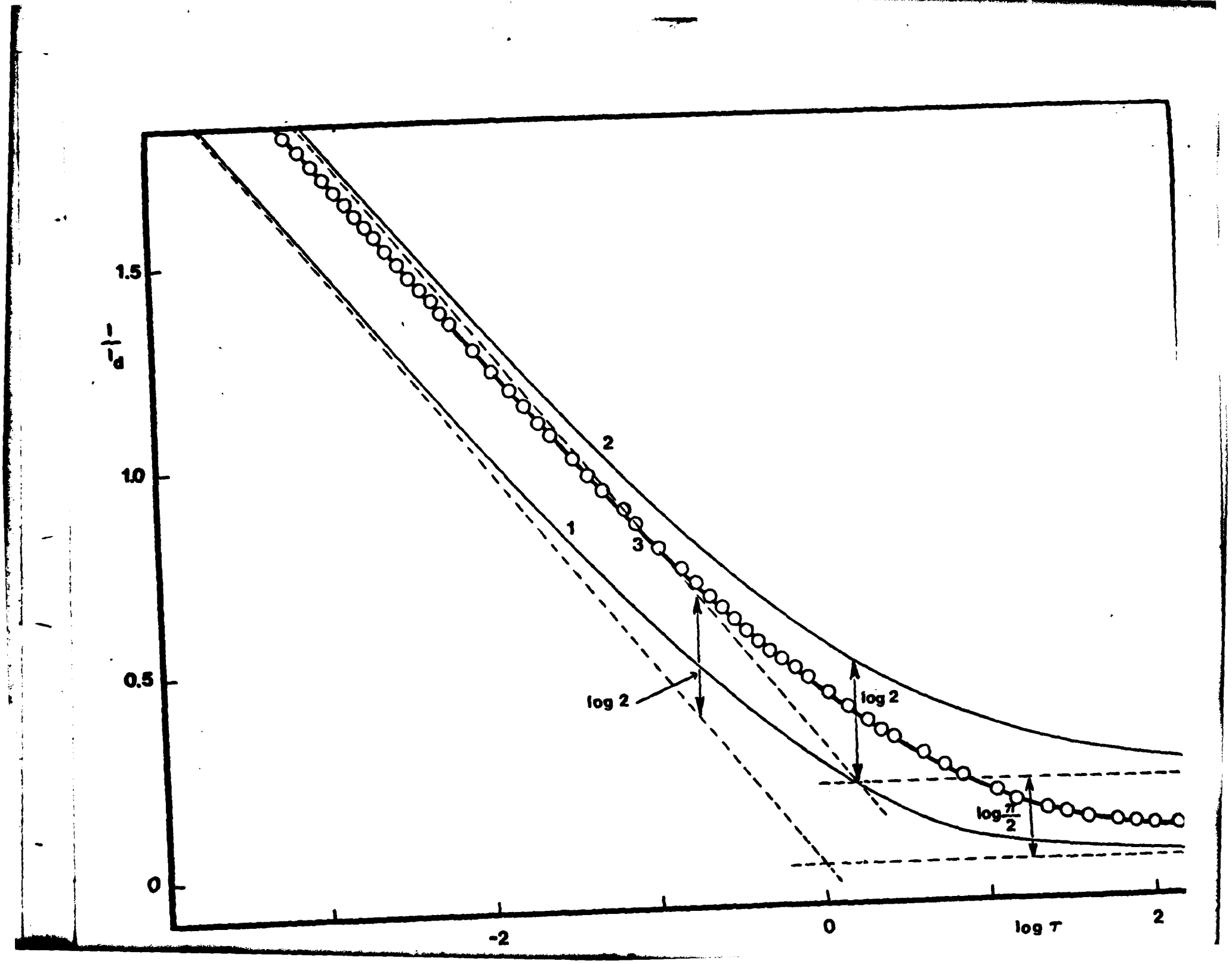
1.5
1.0
0.5
0
$\frac{I}{I_d}$
2
1
3
log 2
log 2
$\log\frac{\pi}{2}$
-2
0
log τ
2

SP472-3/A1

472:GAN:716:enj
78u472-608

TECHNICAL REPORT DISTRIBUTION LIST, GEN

	No. Copies
Office of Naval Research Attn: Code 472 800 North Quincy Street Arlington, Virginia 22217	2
ONR Western Regional Office Attn: Dr. R. J. Marcus 1030 East Green Street Pasadena, California 91106	1
ONR Eastern Regional Office Attn: Dr. L. H. Peebles Building 114, Section D 666 Summer Street Boston, Massachusetts 02210	1
Director, Naval Research Laboratory Attn: Code 6100 Washington, D.C. 20390	1
The Assistant Secretary of the Navy (RE&S) Department of the Navy Room 4E736, Pentagon Washington, D.C. 20350	1
Commander, Naval Air Systems Command Attn: Code 310C (H. Rosenwasser) Department of the Navy Washington, D.C. 20360	1
Defense Technical Information Center Building 5, Cameron Station Alexandria, Virginia 22314	12
Dr. Fred Saalfeld Chemistry Division, Code 6100 Naval Research Laboratory Washington, D.C. 20375	1
U.S. Army Research Office Attn: CRD-AA-IP P.O. Box 1211 Research Triangle Park, N.C. 27709	1
Naval Ocean Systems Center Attn: Mr. Joe McCartney San Diego, California 92152	1
Naval Weapons Center Attn: Dr. A. B. Amster, Chemistry Division China Lake, California 93555	1
Naval Civil Engineering Laboratory Attn: Dr. R. W. Drisko Port Hueneme, California 93401	1
Department of Physics & Chemistry Naval Postgraduate School Monterey, California 93940	1
Scientific Advisor Commandant of the Marine Corps (Code RD-1) Washington, D.C. 20380	1
Naval Ship Research and Development Center Attn: Dr. G. Bosmajian, Applied Chemistry Division Annapolis, Maryland 21401	1
Naval Ocean Systems Center Attn: Dr. S. Yamamoto, Marine Sciences Division San Diego, California 91232	1
Mr. John Boyle Materials Branch Naval Ship Engineering Center Philadelphia, Pennsylvania 19112	1

TECHNICAL REPORT DISTRIBUTION LIST, 359

	No. Copies
Dr. Paul Delahay Department of Chemistry New York University New York, New York 10003	1
Dr. E. Yeager Department of Chemistry Case Western Reserve University Cleveland, Ohio 41106	1
Dr. D. N. Bennion Department of Chemical Engineering Brigham Young University Provo, Utah 84602	1
Dr. R. A. Marcus Department of Chemistry California Institute of Technology Pasadena, California 91125	1
Dr. J. J. Auborn Bell Laboratories Murray Hill, New Jersey 07974	1
Dr. Adam Heller Bell Laboratories Murray Hill, New Jersey 07974	1
Dr. T. Katan Lockheed Missiles & Space Co, Inc. P.O. Box 504 Sunnyvale, California 94088	1
Dr. Joseph Singer, Code 302-1 NASA-Lewis 21000 Brookpark Road Cleveland, Ohio 44135	1
Dr. B. Brummer EIC Incorporated 55 Chapel Street Newton, Massachusetts 02158	1
Library P. R. Mallory and Company, Inc. Northwest Industrial Park Burlington, Massachusetts 01803	1
Dr. P. J. Hendra Department of Chemistry University of Southhampton Southhampton SO9 5NH United Kingdom	1
Dr. Sam Perone Department of Chemistry Purdue University West Lafayette, Indiana 47907	1
Dr. Royce W. Murray Department of Chemistry University of North Carolina Chapel Hill, North Carolina 27514	1
Naval Ocean Systems Center Attn: Technical Library San Diego, California 92152	1
Dr. C. E. Mueller The Electrochemistry Branch Materials Division, Research & Technology Department Naval Surface Weapons Center White Oak Laboratory Silver Spring, Maryland 20910	1
Dr. G. Goodman Globe-Union Incorporated 5757 North Green Bay Avenue Milwaukee, Wisconsin 53201	1
Dr. J. Boechler Electrochimica Corporation Attention: Technical Library 2485 Charleston Road Mountain View, California 94040	1
Dr. P. P. Schmidt Department of Chemistry Oakland University Rochester, Michigan 48063	1
Dr. H. Richtol Chemistry Department Rensselaer Polytechnic Institute Troy, New York 12181	1

TECHNICAL REPORT DISTRIBUTION LIST, 359

	No. Copies
Dr. A. B. Ellis Chemistry Department University of Wisconsin Madison, Wisconsin 53706	1
Dr. M. Wrighton Chemistry Department Massachusetts Institute of Technology Cambridge, Massachusetts 02139	1
Larry E. Plew Naval Weapons Support Center Code 30736, Building 2906 Crane, Indiana 47522	1
S. Ruby DOE (STOR) 600 E Street Washington, D.C. 20545	1
Dr. Aaron Wold Brown University Department of Chemistry Providence, Rhode Island 02192	1
Dr. R. C. Chudacek McGraw-Edison Company Edison Battery Division Post Office Box 28 Bloomfield, New Jersey 07003	1
Dr. A. J. Bard University of Texas Department of Chemistry Austin, Texas 78712	1
Dr. M. M. Nicholson Electronics Research Center Rockwell International 3370 Miraloma Avenue Anaheim, California	1
Dr. Donald W. Ernst Naval Surface Weapons Center Code R-33 White Oak Laboratory Silver Spring, Maryland 20910	1
Dr. R. P. Van Duyne Department of Chemistry Northwestern University Evanston, Illinois 60201	1
Dr. B. Stanley Pons Department of Chemistry University of Alberta Edmonton, Alberta CANADA T6G 2G2	1
Dr. Michael J. Weaver Department of Chemistry Michigan State University East Lansing, Michigan 48824	1
Dr. R. David Rauh EIC Corporation 55 Chapel Street Newton, Massachusetts 02158	1
Dr. J. David Margerum Research Laboratories Division Hughes Aircraft Company 3011 Malibu Canyon Road Malibu, California 90265	1
Dr. Martin Fleischmann Department of Chemistry University of Southampton Southampton 509 5NH England	1
Dr. Janet Osteryoung Department of Chemistry State University of New York at Buffalo Buffalo, New York 14214	1
Dr. R. A. Osteryoung Department of Chemistry State University of New York at Buffalo Buffalo, New York 14214	1
Mr. James R. Moden Naval Underwater Systems Center Code 3632 Newport, Rhode Island 02840	1

TECHNICAL REPORT DISTRIBUTION LIST, 359

	No. Copies
Dr. R. Nowak Naval Research Laboratory Code 6130 Washington, D.C. 20375	1
Dr. John F. Houlihan Shenango Valley Campus Pennsylvania State University Sharon, Pennsylvania 16146	1
Dr. D. F. Shriver Department of Chemistry Northwestern University Evanston, Illinois 60201	1
Dr. D. H. Whitmore Department of Materials Science Northwestern University Evanston, Illinois 60201	1
Dr. Alan Bewick Department of Chemistry The University Southampton, S09 5NH England	1
Dr. A. Himy NAVSEA-5433 NC #4 2541 Jefferson Davis Highway Arlington, Virginia 20362	1
Dr. John Kincaid Department of the Navy Stategic Systems Project Office Room 901 Washington, DC 20376	1
M. L. Robertson Manager, Electrochemical Power Sonices Division Naval Weapons Support Center Crane, Indiana 47522	1
Dr. Elton Cairns Energy & Environment Division Lawrence Berkeley Laboratory University of California Berkeley, California 94720	1
Dr. Bernard Spielvogel U.S. Army Research Office P.O. Box 12211 Research Triangle Park, NC 27709	1
Dr. Denton Elliott Air Force Office of Scientific Research Bolling AFB Washington, DC 20332	1
Dr. David Aikens Chemistry Department Rensselaer Polytechnic Institute Troy, NY 12181	1
Dr. A. P. B. Lever Chemistry Department York University Downsview, Ontario M3J1P3 Canada	1
Mr. Maurice F. Murphy Naval Sea Systems Command 63R32 2221 Jefferson Davis Highway Arlington, VA 20360	1
Dr. Stanislaw Szpak Naval Ocean Systems Center Code 6343 San Diego, CA 95152	1
Dr. Gregory Farrington Department of Materials Science & Engineering University of Pennsylvania Philadelphia, PA 19104	1
Dr. Bruce Dunn Department of Engineering & Applied Science University of California Los Angeles, CA 90024	1

TECHNICAL REPORT DISTRIBUTION LIST, 359

	No. Copies
Dr. Micha Tomkiewicz Department of Physics Brooklyn College Brooklyn, NY 11210	1
Dr. Lesser Blum Department of Physics University of Puerto Rico Rio Piedras, PR 00931	1
Dr. Joseph Gordon II IBM Corporation K33/281 5600 Cottle Road San Jose, CA 95193	1
Dr. Robert Somoano Jet Propulsion Laboratory California Institute of Technology Pasadena, CA 91103	1

END

DATE

FILMED

1-82

DTIC


Cow

AD-A108 567 CHRONOAMPEROMETRIC TRANSIENTS AT THE STATIONARY DISK MICROELECTRODE(U) STATE UNIV OF NEW YORK AT BUFFALO DEPT OF CHEMISTRY T HEPEL ET AL. 30 NOV 81 TR-7

UNCLASSIFIED N00014-79-C-0682 F/G 9/1 NL

2/2

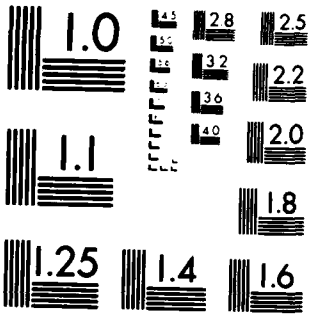

SUPPLEMENTARY

INFORMATION

AD-A126 567

SECURITY CLASSIFICATION OF THIS PAGE (When Data Entered)

REPORT DOCUMENTATION PAGE		READ INSTRUCTIONS BEFORE COMPLETING FORM
1. REPORT NUMBER Technical Report No. 12	2. GOVT ACCESSION NO.	3. RECIPIENT'S CATALOG NUMBER
4. TITLE (and Subtitle) Correction to "Chronoamperometric Transients at the Stationary Disk Microelectrode"		5. TYPE OF REPORT & PERIOD COVERED 6. PERFORMING ORG. REPORT NUMBER
7. AUTHOR(s) Tadeusz Hepel, Wolfgang Plot, and Janet Osteryoung		8. CONTRACT OR GRANT NUMBER(s) N00014-79-C-0682
9. PERFORMING ORGANIZATION NAME AND ADDRESS Department of Chemistry State University of New York at Buffalo		10. PROGRAM ELEMENT, PROJECT, TASK AREA & WORK UNIT NUMBERS NR-056-715
11. CONTROLLING OFFICE NAME AND ADDRESS Office of Naval Research/Chemistry Program Arlington, Virginia 22217		12. REPORT DATE March 2, 1983 13. NUMBER OF PAGES 8
14. MONITORING AGENCY NAME & ADDRESS(if different from Controlling Office)		15. SECURITY CLASS. (of this report) 15a. DECLASSIFICATION/DOWNGRADING SCHEDULE

16. DISTRIBUTION STATEMENT (of this Report)

Approved for Public Release: Distribution Unlimited

17. DISTRIBUTION STATEMENT (of the abstract entered in Block 20, if different from Report)

18. SUPPLEMENTARY NOTES

Prepared for publication in Journal of Physical Chemistry

19. KEY WORDS (Continue on reverse side if necessary and identify by block number)

Chronoamperometric transients; microelectrodes; diffusion coefficients

20. ABSTRACT (Continue on reverse side if necessary and identify by block number)

A previous paper, "Chronoamperometric Transients at the Stationary Disk Microelectrode" by T. Hepel and Janet Osteryoung, relied upon results of previous theoretical work which was subsequently found to have an error. This communication corrects that error and shows that the effect of the error on the work of Hepel and Osteryoung is negligible.

DD FORM 1 JAN 73 1473 EDITION OF 1 NOV 65 IS OBSOLETE

SECURITY CLASSIFICATION OF THIS PAGE (When Data Entered)

OFFICE OF NAVAL RESEARCH

Contract N00014-79-C-0682

Task No. NR-056-715

TECHNICAL REPORT NO. 12

CORRECTION TO "CHRONOAMPEROMETRIC TRANSIENTS AT THE STATIONARY DISK MICROELECTRODE"

by

TADEUSZ HEPEL, WOLFGANG PLOT, AND JANET OSTERYOUNG

Accepted for Publication in

Journal of Physical Chemistry

Department of Chemistry
State University of New York at Buffalo
Buffalo, New York 14214

March, 1983

Correction to "Chronoamperometric Transients at the Stationary Disk Microelectrode"

Sir: Aoki and Osteryoung have reported the solution for chronoamperometric transients at a finite disk electrode[1] and tested the theory experimentally.[2] However, the work of Sato et al.[3] and of Heinze[4] suggested that there might be errors in the solution. Subsequently, Hepel and Osteryoung elaborated on this work.[5] A recent paper by Shoup and Szabo[6] identifies an error in the long-time solution of Aoki and Osteryoung.[1] This error arises from incorrect evaluation of the residue $\Gamma(^1/_4 + Z/2) = 2(-1)^m/m!$ for $Z = -2n - {}^1/_2$, $n = 0, 1, 2, \ldots$. Consequently, the first term for W_p in eq 25 of ref 1 should be multiplied by 2 and the correct long-time expansion of eq 30 of ref 1 is[6]

$$\lim_{\tau_1 \to \infty} f(\tau_1) = 1 + 4\pi^{-3/2}\tau_1^{-1/2} + 32(9^{-1} - \pi^{-2})\pi^{-3/2}\tau_1^{-3/2} + \ldots = 1 + 0.71835\tau_1^{-1/2} + 0.05626\tau_1^{-3/2} - 0.0064558\tau_1^{-5/2} \quad (1)$$

The dimensionless time, τ_1, is given by $\tau_1 = 4Dt/a^2$, where D is the diffusion coefficient (cm^2/s), t the time (s), and a the radius of the electrode (cm). The current is expressed as $I = 4nFDaC^b f(\tau_1)/(1 + \zeta)$ as described previously.[1,5] Equation 1 is accurate for $\tau_1 > 1$ as can be seen by comparison with the empirical solution of ref 6:

$$f(\tau_1) = 0.7854 + 0.8862\tau_1^{-1/2} + 0.2146 \exp(-0.7823\tau_1^{-1/2}) \quad (2)$$

In ref 5 a slightly different definition of the dimensionless time was used:

$$\tau_2 = 16Dt/\pi a^2 = 4\tau_1/\pi \quad (3)$$

The incorrect eq 6 of ref 5

$$f(\tau_2) = 1 + 0.4052847\tau_2^{-1/2} + 0.35412\tau_2^{-3/2} + 0.3785\tau_2^{-5/2} + \ldots \quad (4)$$

should be corrected to

$$f(\tau_2) = 1 + 0.81057\tau_2^{-1/2} + 0.080829\tau_2^{-3/2} - 0.011809\tau_2^{-5/2} + \ldots \quad (5)$$

which fits the empirical solution based on ref 6

$$f(\tau_2) = 0.7854 + \tau_2^{-1/2} + 0.2146 \exp(-0.88273\tau_2^{-1/2}) \quad (6)$$

for $\tau_2 > 1$ as can be seen from Figure 1. Figure 1 also shows the short-term expansion

$$f(\tau_2) = 0.78540 + \tau_2^{-1/2} - 0.0072287\tau_2 - 0.00029108\tau_2^2 + \ldots \quad (7)$$

Note that in contrast to Figure 1 of ref 5, there are no longer two intersections of the short- and long-time solutions. The difference between the short-term expansion (eq 7) and the long-term expansion (eq 5) has the minimum value at $\tau_2 = 0.8623$, $\log \tau = -0.06432$. Thus the Heaviside function of eq 7 of ref 5 should employ 0.9 rather than 3.69 as the crossover point between the two solutions. On the scale of the figure as printed, this change causes a barely preceptible change in Figure 2 of ref 5. The rest of the figures and the treatment of data are unaffected by this error.

Acknowledgment. The authors thank Koichi Aoki for providing the coefficient of the last term of eq 1. This work was supported in part by the Office of Naval Research.

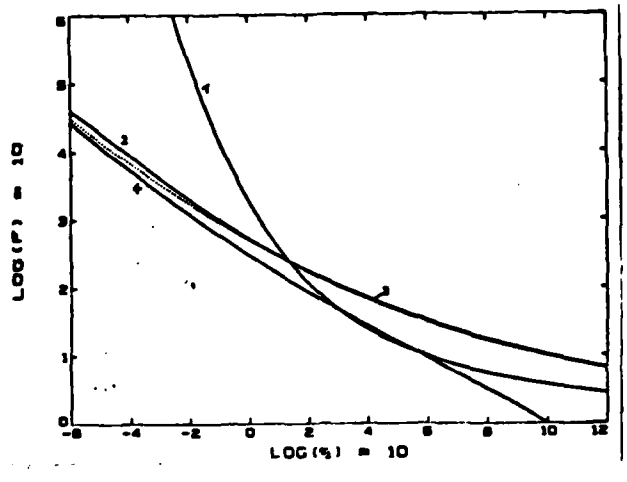

Figure 1. Plots of log $f(\tau_2)$ vs. log τ_2 for (1) incorrect long-time solution, eq 4; (2) corrected long-time solution, eq 5; (3) empirical solution eq 6; (4) short-time solution, eq 7.

(1) Aoki, K.; Osteryoung, Janet *J. Electroanal. Chem.* **1981**, *122*, 19–35.

(2) Aoki, K.; Osteryoung, Janet *J. Electroanal. Chem.* **1981**, *125*, 315–20.

(3) Kakihana, M.; Ikeuchi, H.; Sato, G. P. *J. Electroanal. Chem.* **1981**, *117*, 201.

(4) Heinze, J. *J. Electroanal. Chem.* **1981**, *124*, 73.

(5) Hepel, T.; Osteryoung, Janet *J. Phys. Chem.* **1982**, *86*, 1406–11.

(6) Shoup, D.; Szabo, A. *J. Electroanal. Chem.*, **1982**, *140*, 237–45.

† Institute of Chemistry, Jagiellonian University, 30-060 Krakow, Poland.

Department of Chemistry
State University of New York at Buffalo
Buffalo, New York 14214

Tadeusz Hepel†
Wolfgang Plot
Janet Osteryoung*

Received: July 30, 1982; In Final Form: January 17, 1983


DATE
ILME